

Mapping the Hydration Dynamics of Ubiquitin

Nathaniel V. Nucci, Maxim S. Pometun, and A. Joshua Wand

Johnson Research Foundation and Department of Biochemistry & Biophysics, University of Pennsylvania, 422 Curie Blvd,
Philadelphia, Pennsylvania 191104-6059

Supplementary Information

Materials & Methods

Sample preparation. All isotopically labeled compounds were obtained from Cambridge Isotopes Laboratories (Andover, MA). Unlabeled chemicals were purchased from Sigma-Aldrich (St. Louis, MO). Uniformly ^{15}N , ^{13}C - and ^{15}N , ^2H (99%)-labeled ubiquitin were purified as described previously¹ except that minimal media cultures were supplied with deuterated glucose (*d*-7) and grown in 99% D_2O for uniform ^2H -labeling. The purification protocol involves refolding of ubiquitin, which was performed in H_2O solutions to allow complete exchange of amide deuterons for hydrogens. All reverse micelle samples were made in 75 mM sodium bis-2-ethylhexyl sulfosuccinate (AOT) using 50 mM sodium acetate (*d*-3), pH 5, with 50 mM NaCl.^{2,3} All samples had a measured [water]/[surfactant] ratio (W_0) of 9 ± 0.3 . ^{15}N , ^2H ubiquitin reverse micelle samples were prepared using deuterated pentane (98% *d*-12) as the bulk organic solvent. ^{15}N , ^{13}C -ubiquitin reverse micelle samples were prepared in liquid propane (98% *d*-8) at 600 psi using specialized apparatus from Daedalus Innovations, LLC (Philadelphia, PA). Aqueous ^{15}N , ^{13}C -ubiquitin samples were composed of 1 mM protein, 50 mM sodium acetate (*d*-3), pH 5, and 50 mM NaCl.

NMR spectroscopy. All NMR experiments were performed at 20 °C using Bruker Avance III NMR spectrometers operating at 500 or 600 MHz as indicated and were equipped with cryoprobes. All multidimensional NMR experiments used the States-TPPI^{4,5} method for quadrature detection in the incremented time domain(s) unless otherwise indicated. The spectrometer was locked on the methyl deuterium signal of the alkane solvent for reverse micelle samples or on deuterium oxide for aqueous samples. Standard implementations of the sensitivity-enhanced⁶ ^{15}N -resolved NOESY-HSQC,^{7,9} and non-sensitivity enhanced ^{13}C -resolved NOESY-HSQC implemented with the WET sequence for suppression of AOT resonances in the methyl (1.05 p.p.m. and 0.92 p.p.m.) and methylene (1.35 p.p.m.) regions were used. As noted, in some cases these were recorded as ^{15}N or ^{13}C projections, respectively. For detection of hydration water, matched three-dimensional ^{15}N -resolved ROESY¹⁰⁻¹² and ^{15}N -resolved NOESY spectra were obtained on the same sample. The ROESY experiment employed a 8.33 kHz CW

spin-lock field with the 90x–SLy–90x scheme to minimize spin-lock offset effects¹³. ROESY spectra were recorded on samples prepared in propane for comparison to earlier measurements¹⁴ on samples prepared in pentane. ¹H-¹H projections of the ¹⁵N-resolved NOESY-HSQC were recorded for each sample at 10, 25, 40, and 75 ms NOE mixing time (τ_{mix}) to determine the linear region of the NOE and to characterize long-range dipolar interactions between the protein and alkane solvent. ¹H_N T_{1ρ} values were measured using the ¹⁵N-¹H projection of the three-dimensional ROESY experiment at nine different mixing times ranging from 1 ms to 80 ms with three delays recorded in duplicate for error analysis. NOE/ROE ratios were calculated for those sites which were well resolved from H_α cross peaks as described previously,¹⁴ and differences from the previously published values were found to be within measurement error (data not shown).

Experiments to measure hydration near aliphatic hydrogens employed the corresponding ¹³C-resolved NOESY-HSQC and ROESY-HSQC experiments and were recorded on ¹⁵N,¹³C-ubiquitin in reverse micelles in perdeuterated liquid propane (*d*-8) at 600 MHz using 16 transients, 40 complex increments with gradient selection for quadrature in the indirect ¹³C dimension, and 64 complex increments with States-TPPI quadrature detection in the indirect ¹H dimension. ¹H_C T_{1ρ} values were measured from the ¹³C-¹H projection of the three-dimensional ¹³C-resolved ROESY experiment at nine different mixing times ranging from 1 ms to 35 ms with three delays recorded in duplicate for error analysis. ¹³C - ROESY experiments employed a 10 kHz CW spin-lock field with the 90x–SLy–90x scheme. The spin-lock pulse carrier frequency was moved to -1.0 p.p.m. in order to prevent HOHAHA transfers¹⁵ from contributing to the measured cross peaks. For comparison to the reverse micelle spectra, ¹³C-resolved NOESY-HSQC and ROESY-HSQC experiments were recorded on ¹⁵N,¹³C-ubiquitin in aqueous solution at 600 MHz using 32 transients, 32 complex increments with gradient selection in the indirect ¹³C dimension and 50 complex increments in the indirect ¹H dimension. The ROESY spin lock was performed as for the reverse micelle sample.

NMR Data Analysis. Spectra were processed with FELIX (Accelrys, San Diego, CA) and analyzed with Sparky.¹⁶ $T_{1\rho}$ values were determined by fitting intensity decays to single exponential functions using NumPy in Python 2.5. NOE/ROE values were calculated using:¹⁷

$$\frac{\sigma_{NOE}}{\sigma_{ROE}} = \frac{NOE}{ROE} e^{-\frac{\tau_{mix}}{T_{1\rho}}} \quad (1)$$

Where NOE and ROE denote simple maximum peak intensities. In a minority of cases, resolution was insufficient for intensities to be used. In these cases, peaks were fit in SPARKY¹⁶ to determine peak volumes, which were used in place of intensities. The spectral parameter used is indicated in Table 1 where the $\sigma_{NOE}/\sigma_{ROE}$ ratios are reported.

Molecular modeling and analysis. PyMol (Schrödinger, Portland) was used to create molecular images and to overlay molecular structures for analysis of crystallographic waters and for analysis of ubiquitin complexes. The reverse micelle model was created using CNS¹⁸ and visualized using PyMol. Burial depth of each hydration dynamic probe was calculated using the Travel Depth^{19,20} suite of programs and was averaged over the 32 structures in the reverse micelle ubiquitin NMR structural ensemble (PDB ID 1G6J²). The Cartesian coordinates of the Lee-Richards²¹ solvent-accessible molecular surface (SAS) generated by the Travel Depth suite for conformer 25 of the 1G6J ensemble were used to compute the hydration dynamic map of the ubiquitin surface. The distance from each point on the SAS to each hydration dynamics probe was calculated. Each point that was within NOE distance of one or more hydration dynamic probes was assigned an NOE/ROE value corresponding to the simple average of the NOE/ROE values for all of the probes within NOE distance of it. Surface points outside NOE distance from any hydration dynamic probe were not assigned a value. For this analysis, the present ¹³C-resolved NOE/ROE values were combined with the previously published ¹⁵N-resolved values obtained in liquid pentane. The NOE maximum distances used were: 3.25 Å for C-Hs, corresponding to the maximum ¹³C-resolved NOE distance at 35 ms τ_{mix} as calibrated using intramolecular NOEs; 4.25 Å for sites where the position of the carbon atom was used rather than the hydrogen position due to degeneracy of attached

hydrogen chemical shifts, corresponding to the calibrated NOE distance plus 1 Å for the C-H bond; and 4.55 Å for N-Hs, corresponding to the maximum detectable NOE distance calibrated previously.¹⁴

Comparison of sites of NMR-detected restricted hydration dynamics with crystallographic water locations was performed by aligning conformer 25 of the reverse micelle ubiquitin structural ensemble (PDB ID 1G6J²) with two room temperature crystal structures of ubiquitin (PDB IDs 1UBQ²² and 1UBI²³). Distances between sites were calculated in PyMol. Comparison of crystal structures of ubiquitin complexes was performed using PyMOL. Conformer 25 of the reverse micelle NMR structural ensemble (PDB ID 1G6J) was aligned with each of the 20 ubiquitin complexes previously analyzed by Lange et al.²⁴ Details regarding which structures were used are given Table S2.

Analysis of ubiquitin complexes. Eighteen crystal structures of heteromolecular ubiquitin binding complexes were used to examine if there was a correlation between the nature of ubiquitin hydration dynamics and the ubiquitin binding interfaces. The complexes and their PDB ID codes and references are given in Table S2. One ubiquitin molecule in each complex was aligned with conformer 25 of the reverse micelle ubiquitin structural ensemble (PDB ID 1G6J)² using PyMOL (Schrödinger, Portland). All non-ubiquitin heavy atoms within 6 Å of conformer 25 of 1G6J were considered to be interfacial atoms of the ubiquitin binding partners. These atoms are those shown as spheres in Figure 3 of the main text.

Table S1. Apparent hydration water $\sigma_{\text{NOE}}/\sigma_{\text{ROE}}$ values and $T_{1\rho}$ relaxation time constants for ^1H - ^{13}C probes of hydration in ubiquitin.

Assignment	$\sigma_{\text{NOE}}/\sigma_{\text{ROE}}$ (± 0.05)	$T_{1\rho}$ (s)	Assignment	$\sigma_{\text{NOE}}/\sigma_{\text{ROE}}$ (± 0.05)	$T_{1\rho}$ (s)	Assignment	$\sigma_{\text{NOE}}/\sigma_{\text{ROE}}$ (± 0.05)	$T_{1\rho}$ (s)
K33 H $_{\gamma}$ 2/3	-0.53	0.0400	T14 H $_{\gamma}$ 2*	-0.37	0.0292	R74 H $_{\beta}$ 2*	-0.16	0.0188
T7 H $_{\beta}$	-0.49	0.0187	L69 H $_{\beta}$ 2	-0.33	0.0248	D32 H $_{\beta}$ 3*	-0.15	0.0210
T22 H $_{\alpha}$	-0.47	0.0184	I13 H $_{\gamma}$ 2	-0.29	0.0289	K11 H $_{\beta}$ 3*	-0.14	0.0203
T7 H $_{\alpha}$	-0.47	0.0239	P19 H $_{\beta}$ 3	-0.28	0.0182	P37 H $_{\beta}$ 3	-0.12	0.0187
K6 H $_{\delta}$ 2/3*	-0.47	0.0299	K33 H $_{\beta}$ 2	-0.27	0.0184	K33 H $_{\beta}$ 3*	-0.10	0.0237
T9 H $_{\beta}$	-0.45	0.0273	K63 H $_{\beta}$ 3*	-0.27	0.0207	Q62 H $_{\beta}$ 3	-0.09	0.0192
K33 H $_{\delta}$ 2/3*	-0.45	0.0448	M1 H $_{\beta}$ 3	-0.26	0.0194	Q31 H $_{\gamma}$ 3	-0.09	0.0184
R72 H $_{\gamma}$ 2/3*	-0.43	0.0172	F4 H $_{\beta}$ 2/3*	-0.25	0.0198	F45 H $_{\delta}$	-0.05	0.0261
K29 H $_{\eta}$ 3*	-0.42	0.0438	Q49 H $_{\gamma}$ 2	-0.24	0.0229	Q2 H $_{\gamma}$ 3*	-0.04	0.0255
L8 H $_{\delta}$ 2	-0.42	0.0442	M1 H $_{\beta}$ 2	-0.21	0.0168	Q2 H $_{\beta}$ 3	NQ	0.0210
M1 H $_{\gamma}$ 2*	-0.39	0.0221	K29 H $_{\beta}$ 3	-0.21	0.0155	E18 H $_{\beta}$ 3	NQ	0.0203
K11 H $_{\delta}$ 2/3	-0.38	0.0359	K29 H $_{\beta}$ 2	-0.20	0.0168	K33 H $_{\eta}$	NQ	0.0400
T9 H $_{\gamma}$ 2*	-0.38	0.0293	K63 H $_{\eta}$ 2/3*	-0.18	0.0373	R42 H $_{\gamma}$ 2/3	NQ	0.0176
Q41 H $_{\beta}$ 2*	-0.38	0.0178	Q62 H $_{\beta}$ 2*	-0.17	0.0194	I44 H $_{\gamma}$ 2	NQ	0.0254

$\sigma_{\text{NOE}}/\sigma_{\text{ROE}}$ values were calculated as described in Materials and Methods. *indicates sites for which fitted peak volumes were used in lieu of intensities. NQ indicates sites which were not quantitative, representing sites where cross relaxation to water was observed but was not quantified due to insufficient quality of the data. In most cases, this was the result of overlap with surfactant signals. Error for $T_{1\rho}$ was less $\leq 2\%$ for all sites.

Table S2. Crystal structures used for analysis ubiquitin heteromolecular complexes.

PDB ID	Ubiquitin Binding Partner	Reference
2G45	Zinc-finger ubiquitin-binding domain of isopeptidase T (USP5)	25
1CMX	Yeast ubiquitin C-terminal hydrolase, Yuhl	26
1NBF	UBP-family deubiquitinating enzyme	27
1OTR	Yeast Cue 2 protein	28
1P3Q	Vacuolar protein sorting-associated protein VPS9P, Cue domain	29
1S1Q	Vacuolar protein sorting-associated protein TSG101, UEV domain	30
1UZX	Vacuolar protein sorting-associated protein VPS23	31
1WR1	Ubiquitin-associated domain of Dsk2p	32
1WR6	Human GGA3 C-GAT	33
1WRD	GAT domain of Tom-1	34
1XD3	Human ubiquitin C-terminal hydrolase, L3	35
1YD8	GAT domain of human GGA3	36
2AYO	Ubiquitin-specific processing protease, USP14	37
2C7M	Guanine nucleotide-exchange factor, Rabex-5	38
2C7N	Guanine nucleotide-exchange factor, Rabex-5	38
2D3G	Ubiquitin-interacting motif of Hrs	39
2FID	Guanine nucleotide-exchange factor, Rabex-5	40
2FIF	Guanine nucleotide-exchange factor, Rabex-5	40

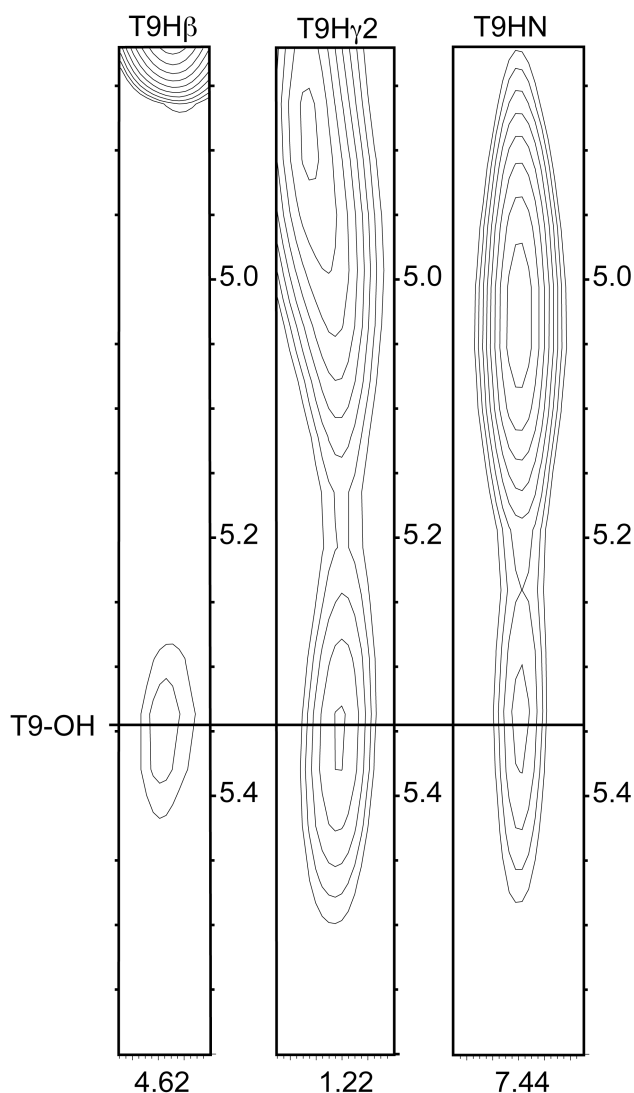


Figure S1. Intramolecular cross peaks to side chain hydroxyl hydrogens. Cross peaks are shown in ^1H - ^1H strip plots from ^{13}C - and ^{15}N -resolved NOESY spectra with the directly-detected dimension on the abscissa and the indirect ^1H dimension on the ordinate axis. These cross peaks are to the hydroxyl hydrogen of Thr-9 demonstrating that the hydroxyl hydrogen is resolved from the water resonance and therefore in slow exchange. The slight variation in chemical shift of the cross peak is within the digital resolution of the spectra. This and similar interactions involving other side chain hydroxyl hydrogens demonstrate that hydrogen exchange in reverse micelles is effectively quenched by more than two orders of magnitude relative to free aqueous solution.

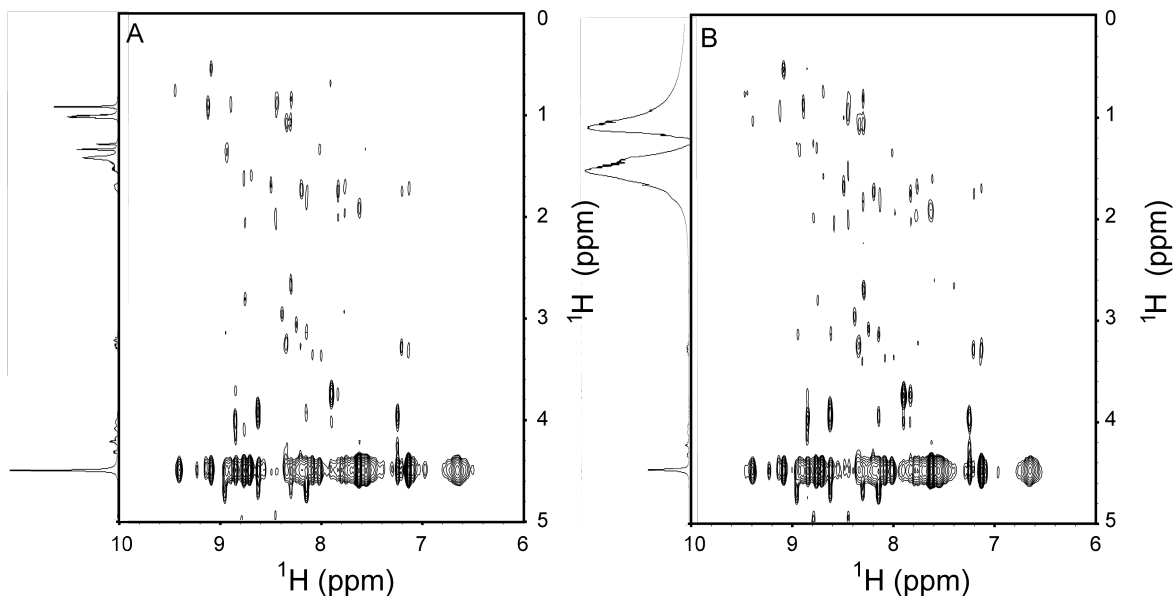


Figure S2. Demonstration of the absence of long-range protein-alkane solvent dipolar coupling. ^1H - ^1H NOESY projections of ^{15}N -resolved NOESY experiments are shown for uniformly ^{15}N , ^2H -labeled ubiquitin encapsulated in AOT reverse micelles in (A) 98% perdeuterated pentane or in (B) 10% perdeuterated, 90% ^1H -pentane. One-dimensional ^1H spectra of each sample are shown vertically on the left of each spectrum. The contribution of the ^1H -pentane in (B) is evident in the one-dimensional spectrum yet no increase in cross peak intensity is seen in the NOESY projection. This confirms the absence of long-range coupling between the protein and alkane solvent hydrogens.

References

- (1) Peterson, R. W.; Pometun, M. S.; Shi, Z.; Wand, A. J. *Protein Sci* 2005, 14, 2919.
- (2) Babu, C. R.; Flynn, P. F.; Wand, A. J. *J. Am. Chem. Soc.* 2001, 123, 2691.
- (3) Wand, A. J.; Ehrhardt, M. R.; Flynn, P. F. *Proc. Natl. Acad. Sci. U. S. A.* 1998, 95, 15299.
- (4) Marion, D.; Wuthrich, K. *Biochem. Biophys. Res. Comm.* 1983, 113, 967.
- (5) States, D. J.; Haberkorn, R. A.; Ruben, D. J. *J. Magn. Reson.* 1982, 48, 286.
- (6) Palmer, A. G., III; Cavanagh, J.; Wright, P. E.; Rance, M. J. *Magn. Reson.* 1991, 93, 151.
- (7) Kay, L. E.; Keifer, P.; Saarinen, T. *J. Am. Chem. Soc.* 1992, 114, 10663.
- (8) Schleucher, J.; Schwendinger, M.; Sattler, M.; Schmidt, P.; Schedletzky, O.; Glaser, S. J.; Sorensen, O. W.; Griesinger, C. *J. Biomol. NMR* 1994, 4, 301.
- (9) Zhang, O.; Kay, L. E.; Olivier, J. P.; Forman-Kay, J. D. *J. Biomol. NMR* 1994, 4, 845.
- (10) Bax, A.; Davis, D. G. *J. Magn. Reson.* 1985, 63, 207.
- (11) Bothner-By, A. A.; Stephens, R. L.; Lee, J.; Warren, C. D.; Jeanloz, R. W. *J. Am. Chem. Soc.* 1984, 106, 811.
- (12) Clore, G. M.; Bax, A.; Wingfield, P. T.; Gronenborn, A. M. *Biochemistry* 1990, 29, 5671.
- (13) Griesinger, C.; Ernst, R. R. *J. Magn. Reson.* 1987, 75, 261.
- (14) Nucci, N. V.; Pometun, M. S.; Wand, A. J. *Nat. Struct. Mol. Biol.* 2011, 18, 245.
- (15) Desvaux, H.; Berthault, P.; Birlirakis, N.; Goldman, M. J. *Magn. Reson. Series A* 1994, 108, 219.
- (16) Goddard, T. D.; Kneller, D. G.; University of California, San Francisco: San Francisco, CA.
- (17) Macura, S.; Huang, Y.; Suter, D.; Ernst, R. R. *Journal of Magnetic Resonance* 1981, 43, 259.
- (18) Brunger, A. T.; Adams, P. D.; Clore, G. M.; DeLano, W. L.; Gros, P.; Grosse-Kunstleve, R. W.; Jiang, J. S.; Kuszewski, J.; Nilges, M.; Pannu, N. S.; Read, R. J.; Rice, L. M.; Simonson, T.; Warren, G. L. *Acta Crystall.* 1998, D54, 905.
- (19) Coleman, R. G.; Sharp, K. A. *J. Mol. Biol.* 2006, 362, 441.
- (20) Coleman, R. G.; Sharp, K. A. *Proteins* 2009, 78.
- (21) Lee, B.; Richards, F. M. *J. Mol. Biol.* 1971, 55, 379.

- (22) Vijay-Kumar, S.; Bugg, C. E.; Cook, W. J. *J. Mol. Biol.* 1987, 194, 531.
- (23) Alexeev, D.; Bury, S. M.; Turner, M. A.; Ogunjobi, O. M.; Muir, T. W.; Ramage, R.; Sawyer, L. *Biochem. J.* 1994, 299, 159.
- (24) Lange, O. F.; Lakomek, N. A.; Fares, C.; Schroder, G. F.; Walter, K. F. A.; Becker, S.; Meiler, J.; Grubmuller, H.; Griesinger, C.; de Groot, B. L. *Science* 2008, 320, 1471.
- (25) Reyes-Turcu, F. E.; Horton, J. R.; Mullally, J. E.; Heroux, A.; Cheng, X. D.; Wilkinson, K. D. *Cell* 2006, 124, 1197.
- (26) Johnston, S. C.; Riddle, S. M.; Cohen, R. E.; Hill, C. P. *Embo Journal* 1999, 18, 3877.
- (27) Hu, M.; Li, P. W.; Li, M. Y.; Li, W. Y.; Yao, T. T.; Wu, J. W.; Gu, W.; Cohen, R. E.; Shi, Y. G. *Cell* 2002, 111, 1041.
- (28) Kang, R. S.; Daniels, C. M.; Francis, S. A.; Shih, S. C.; Salerno, W. J.; Hicke, L.; Radhakrishnan, I. *Cell* 2003, 113, 621.
- (29) Prag, G.; Misra, S.; Jones, E. A.; Ghirlando, R.; Davies, B. A.; Horazdovsky, B. F.; Hurley, J. H. *Cell* 2003, 113, 609.
- (30) Sundquist, W. I.; Schubert, H. L.; Kelly, B. N.; Hill, G. C.; Holton, J. M.; Hill, C. P. *Mol. Cell* 2004, 13, 783.
- (31) Teo, H.; Vepintsev, D. B.; Williams, R. L. *J. Biol. Chem.* 2004, 279, 28689.
- (32) Ohno, A.; Jee, J.; Fujiwara, K.; Tenno, T.; Goda, N.; Tochio, H.; Kobayashi, H.; Hiroaki, H.; Shirakawa, M. *Structure* 2005, 13, 521.
- (33) Kawasaki, M.; Shiba, T.; Shiba, Y.; Yamaguchi, Y.; Matsugaki, N.; Igarashi, N.; Suzuki, M.; Kato, R.; Kato, K.; Nakayama, K.; Wakatsuki, S. *Genes to Cells* 2005, 10, 639.
- (34) Akutsu, M.; Kawasaki, M.; Katoh, Y.; Shiba, T.; Yamaguchi, Y.; Kato, R.; Kato, K.; Nakayama, K.; Wakatsuki, S. *Febs Letters* 2005, 579, 5385.
- (35) Misaghi, S.; Galardy, P. J.; Meester, W. J. N.; Ovaa, H.; Ploegh, H. L.; Gaudet, R. J. *Biol. Chem.* 2005, 280, 1512.
- (36) Prag, G.; Lee, S. H.; Mattera, R.; Arighi, C. N.; Beach, B. M.; Bonifacino, J. S.; Hurley, J. H. *Proc. Nat. Acad. Sci. U.S.A.* 2005, 102, 2334.
- (37) Hu, M.; Li, P. W.; Song, L.; Jeffrey, P. D.; Chernova, T. A.; Wilkinson, K. D.; Cohen, R. E.; Shi, Y. G. *EMBO J.* 2005, 24, 3747.
- (38) Penengo, L.; Mapelli, M.; Murachelli, A. G.; Confalonieri, S.; Magri, L.; Musacchio, A.; Di Fiore, P. P.; Polo, S.; Schneider, T. R. *Cell* 2006, 124, 1183.
- (39) Hirano, S.; Kawasaki, M.; Ura, H.; Kato, R.; Raiborg, C.; Stenmark, H.; Wakatsuki, S. *Nature Struct. Mol. Biol.* 2006, 13, 272.
- (40) Lee, S.; Tsai, Y. C.; Mattera, R.; Smith, W. J.; Kostelansky, M. S.; Weissman, A. M.; Bonifacino, J. S.; Hurley, J. H. *Nature Struct. Mol. Biol.* 2006, 13, 264.